Memoirs of the Faculty of Engineering, Kyushu University, Vol.67, No.4, December 2007

Axisymmetric Viscous Flow Modeling for Meridional Flow Calculation in Aerodynamic Design of Half-Ducted Blade Rows

by

Soichiro TABATA*, Fumito HIRATANI** and Masato FURUKAWA***

(Received November 5, 2007)

Abstract

A flow modeling for the meridional flow calculation in the aerodynamic design of the half-ducted turbomachinery blade rows has been presented. It is assumed that the meridional flow is axisymmetric and viscous one. To take into account the blade loading, a blade force is introduced as a body force to the axisymmeric Navier-Stokes equations. The blade force contains the inviscid blade effect only, namely, the pressure difference across a blade. Numerical examples have been presented for a wind-lens turbine and a half-ducted propeller fan in order to demonstrate the validity of the present flow modeling. For the wind-lens turbine, the present flow modeling can predict non-uniform flow distributions at the inlet and outlet of the turbine rotor. For the half-ducted propeller fan, however, the formation of the several separated and vortical flow structures results in the well prediction of the inlet flow angle only. It is found that the present flow modeling is useful to the blade row design tool.

Keywords: Turbomachinery, Half-ducted blade row, Meridional flow, Axisymmetric viscous flow, Blade force

1. Introduction

The flow field around half-ducted turbomachinery, for example, propeller fan, has internal and external flow feature, thus being very complicated. It is difficult to design the half-ducted turbomachinery blade rows. For the propeller fans as shown in **Fig. 1**, which are widely used as cooling fans in the outdoor unit of split room air-conditioners, in the cooling unit of engine block on automobiles and in the digital appliance, the shroud wall covers only the rear region of their rotor tips. It has been found that the interaction between the internal and external flows caused complex vortical flow phenomena in the propeller fans[1,2]. In recent, the new concept of wind

*** Professor, Department of Mechanical Engineering Science
** Graduate Student, Department of Mechanical Engineering Science
* Graduate Student, Department of Mechanical Engineering Science

turbine, the wind-lens turbine, has been developed by Kyushu University[3,4]. As shown in **Fig. 2**, the wind-lens turbine has a diffuser with brim, by which the wind concentration to the turbine and the significant enhancement of the turbine output can be achieved. It has been found that the wind concentration effect of the brimmed diffuser is dominated by separated vortical flow around it[4].

As mentioned above, the internal flow in the half-ducted turbomachinery blade row is strongly affected by the external flow around it. Distributions of the meridional flow are not uniform at the inlet and outlet of the half-ducted blade rows, as shown in **Fig. 3** where meridional streamlines and axial velocity distributions are denoted by black lines and color contours, respectively. It is important to take account of the meridional flow distributions in the aerodynamic design of the blade rows. However, it is difficult to predict the inlet and outlet flow distributions affected by meridional streamline curvature and separated vortical flow in the external flow field.

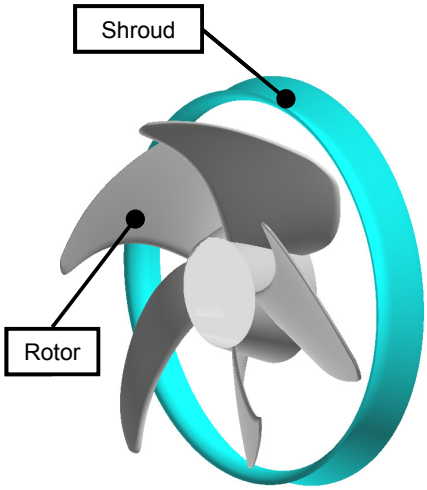

Fig. 1 Half-ducted propeller fan.

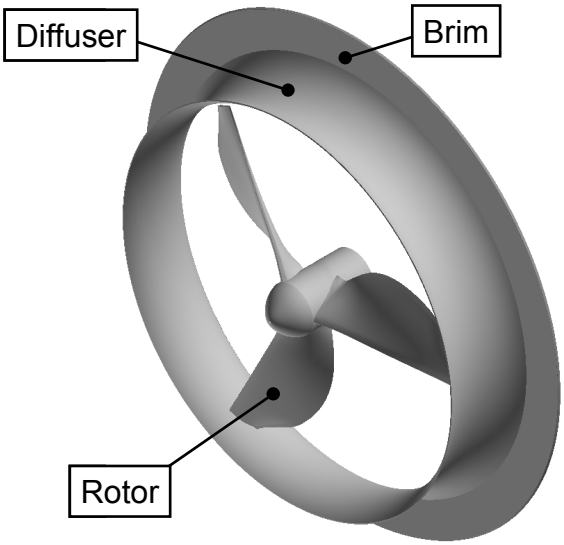

Fig. 2 Wind-lens turbine.

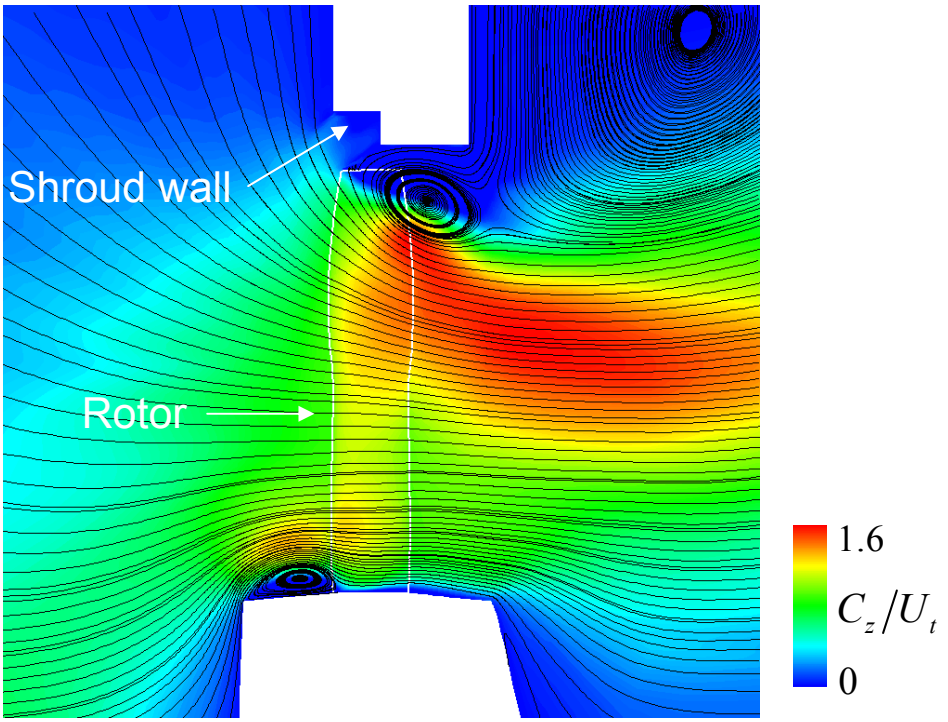

(a) Propeller fan

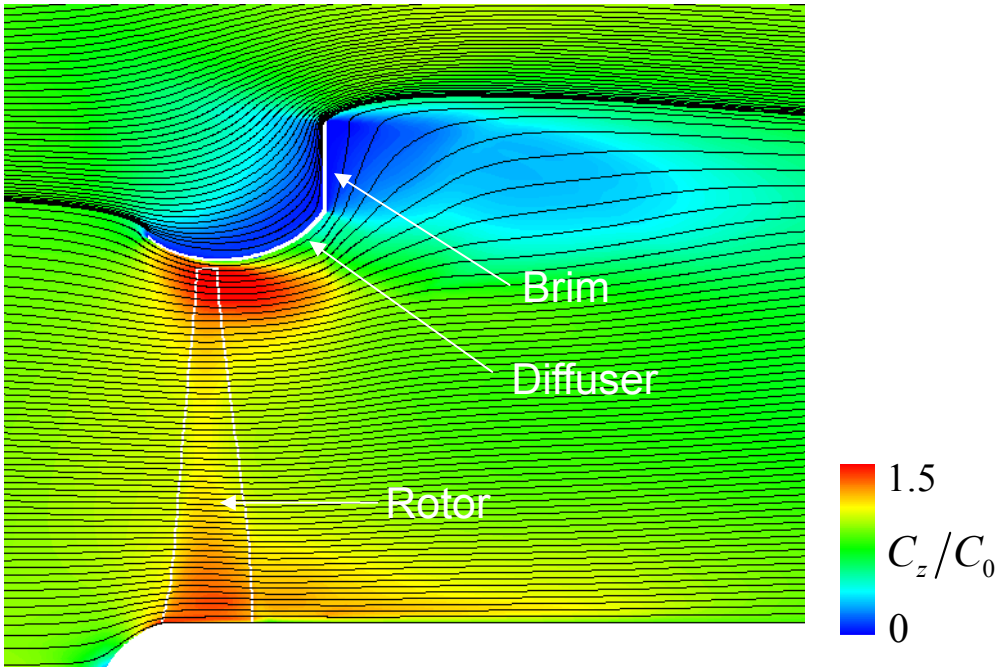

(b) Wind-lens turbine

Fig. 3 Meridional streamlines and axial velocity distributions (three-dimensional computation).

In the present study, an axisymmetric viscous flow modeling for the meridional flow calculation in the aerodynamic design of the half-ducted blade rows is presented. Numerical examples are shown for a wind-lens turbine and a half-ducted propeller fan in order to demonstrate the validity of the present modeling.

2. Flow Modeling

2.1 Blade force

A flow modeling of the meridional flow calculation suitable for the aerodynamic design of the half-ducted turbomachinery blade rows will be described in the following. It is assumed that the meridional flow is axisymmetric and viscous one. As a result, governing equations are besed on the axisymmeric Navier-Stokes equations. To take into account the blade loading on the assumption of the axisymmetric flow, a blade force is introduced as a body force to the governing equations. In the present modeling, the blade force contains the inviscid blade effect only, namely, the pressure difference between the pressure and suction surfaces of a blade.

The blade force is formulated by the inviscid momentum equations, that is, the Euler equations. The following relation[5] is obtained by averaging the circumferential inviscid momentum equation in the circumferential direction, together with the continuity equation.

$$\Delta p = \frac{2\pi K_b}{N} \rho c_m \frac{\partial}{\partial m}\left(r c_\theta\right) \tag{1}$$

Here Δp denotes the pressure difference across the blade, c_m and c_θ represent the meridional and circumferential components of the absolute velocity, respectively, m is the distance along the meridional streamline, ρ is the density of fluid, N is the number of blade, and K_b is the circumferential blockage factor due to the blade. All the flow quantities in the right hand side of the above equation are given as circumferentially averaged values. The above equation relates the pressure difference across the blade with the blade loading, that is, the change in the angular momentum along the meridional streamline.

An apparent blade force is introduced by defining a body force from the pressure difference across the blade, Δp. The circumferential component of the blade force, F_θ, is defined as

$$F_\theta = \frac{\Delta p \cdot dr \cdot dm}{\frac{2\pi}{N} K_b r \cdot dr \cdot dm} = \frac{\Delta p}{\frac{2\pi}{N} K_b r} \tag{2}$$

where r is the radius from the axis of blade row rotation. Using Eqs. (1) and (2), the circumferential component of the blade force can be written as

$$F_\theta = \rho \frac{c_m}{r} \frac{\partial}{\partial m}\left(r c_\theta\right) \tag{3}$$

For the design problem of blade row, the distribution of the blade loading, rc_θ, is given as a design condition.

It is assumed that the blade force acts perpendicularly on the blade camber, because the blade force introduced in the present flow modeling includes no viscous force acting on the blade. The axial and radial components of the blade force, F_z and F_r, can be given as

$$F_z = \frac{n_z}{n_\theta} F_\theta, \qquad F_r = \frac{n_r}{n_\theta} F_\theta \tag{4}$$

where n_z, n_r and n_θ denote the axial, radial and circumferential components of the unit vector normal to the blade camber.

2.2 Numerical scheme

Reynolds averaged axisymmetric Navier-Stokes equations including the blade force mentioned above are solved by an unfactored implicit upwind relaxation scheme[6]. The governing equations are discretized in space using a cell-centered finite volume formulation and in time using the Euler implicit method. The inviscid fluxes are evaluated by a high-resolution upwind scheme based on a TVD formulation[7], where a Roe's approximate Riemann solver and a third-order accurate MUSCL approach are implemented. The viscous fluxes are determined in a central differencing manner with Gauss's theorem. The k-ω two-equation turbulence model of Wilcox[8] is employed to estimate the eddy viscosity. Simultaneous equations linearized in time are solved by a point Gauss-Seidel relaxation method using no approximate factorisation[6]. The no-slip and adiabatic conditions are applied to solid walls with no wall function method.

Boundaries of the computational domain are formed by cell interfaces in the present numerical scheme where the cell-centered finite volume approach is applied to the spatial discretization. Fictitious cells are introduced just outside all the boundaries to treat boundary conditions. Values of conserved variables satisfying the boundary conditions are given at the fictitious cells. Using the fictitious cells, numerical fluxes through the boundaries are evaluated in the same way as interior cell interfaces. This treatment of the boundary conditions prevents nonphysical reflections at the inflow and outflow boundaries, because the inviscid fluxes through the boundaries are evaluated according to the approximate Riemann solver in which the signal propagation properties of the Euler equations are simulated. Details of the boundary conditions can be found from the previous study of Furukawa et al.[9].

3. Numerical Examples

3.1 Wind-lens turbine

The present flow modeling has been applied to a wind-lens turbine to show its validity. The wind-lens turbine has a brimmed diffuser as shown in **Fig. 2**. The wind-lens turbine was designed by a two-dimensional rotor element theory based on the momentum theorem of ducted turbine. Its design specifications are given in **Table 1**. Computational results using the axisymmetric viscous flow modeling were compared with ones of a three-dimensional flow calculation. For the axisymmetric viscous flow calculation, the distribution of the rotor blade loading, rc_θ, was specified by numerical results of the three-dimensional flow calculation. A computational grid used for the axisymmetric viscous flow calculation is shown in **Fig. 4**, which has 39,696 computational cells. On the other hand, a computational grid for the three-dimensional flow calculation has 3,810,336 cells.

Table 1 Design specifications of wind-lens turbine.

Wind approach velocity	**10 [m/s]**
Blade number	**3**
Tip speed ratio	**3.5**
Rotational speed	**670 [rpm]**
Rotor diameter	**1000 [mm]**
Hub/tip ratio	**13.9 [%]**

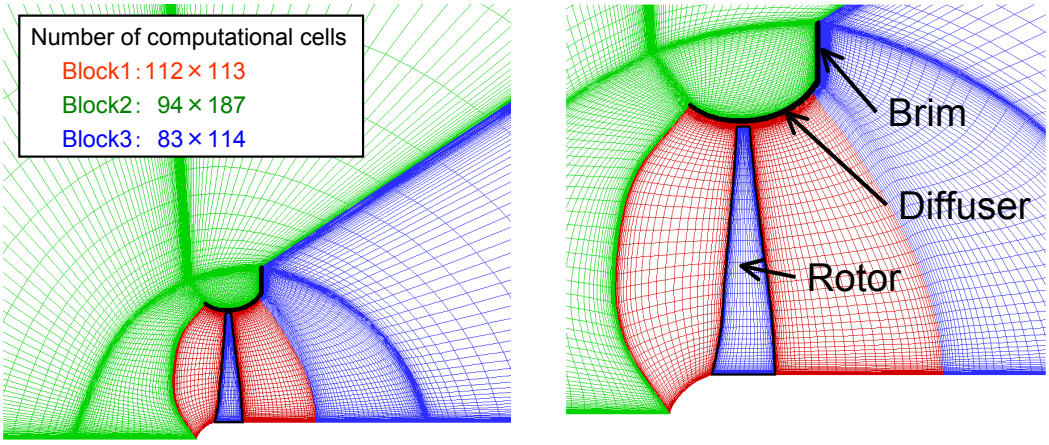

(a) Total view (b) Rotor region

Fig. 4 Computational grid for wind-lens turbine.

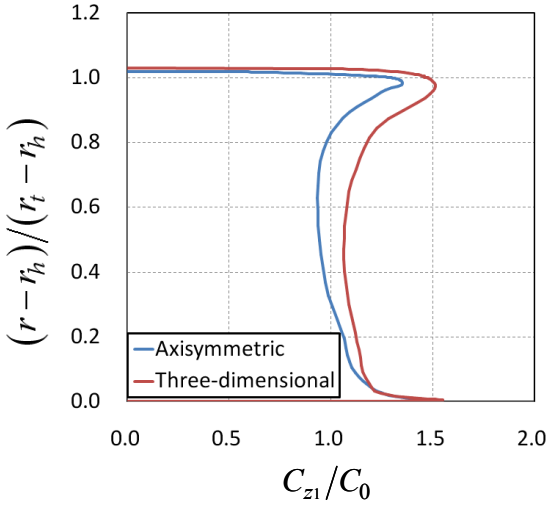

(a) Rotor inlet

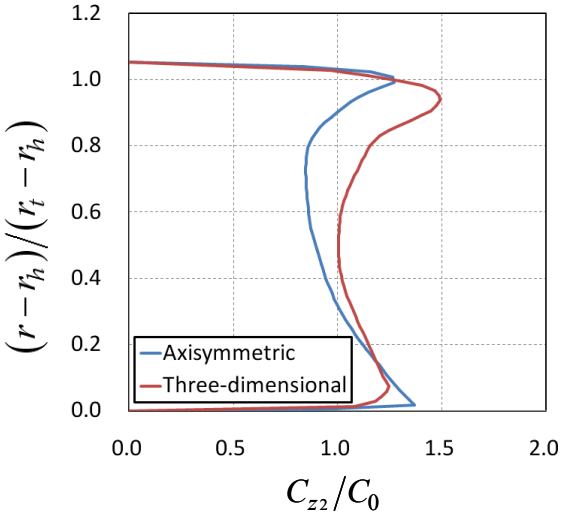

(b) Rotor outlet

Fig. 5 Spanwise distributions of axial velocity for wind-lens turbine.

Figure 5 shows spanwise distributions of the axial velocity at the inlet and outlet of the turbine rotor, where the axial velocity is normalized by the wind approach velocity far upstream of the rotor, and r_h and r_t denote the radii of the hub and rotor tip, respectively. Results of the three-dimensional flow calculation are averaged in the circumferential direction. It is found that the axisymmetric viscous flow calculation can predict non-uniform flow distributions at the inlet and outlet of the rotor. However, a flow rate through the brimmed diffuser is underestimated for the axisymmetric viscous flow calculation.

Spanwise distributions of the relative flow angle measuring from the meridional plane are shown in **Fig. 6**. The distributions are well predicted by the axisymmetric viscous flow calculation. For the inlet flow angle distribution shown in **Fig. 6 (a)**, which is a very important design parameter, the excellent agreement is observed between the axisymmetric and three-dimensional flow calculations.

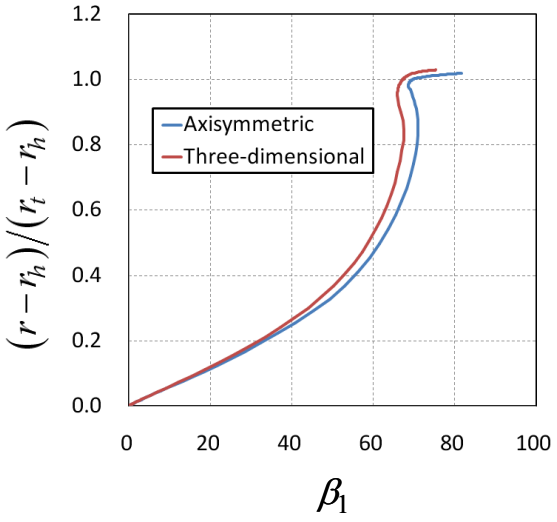

(a) Rotor inlet

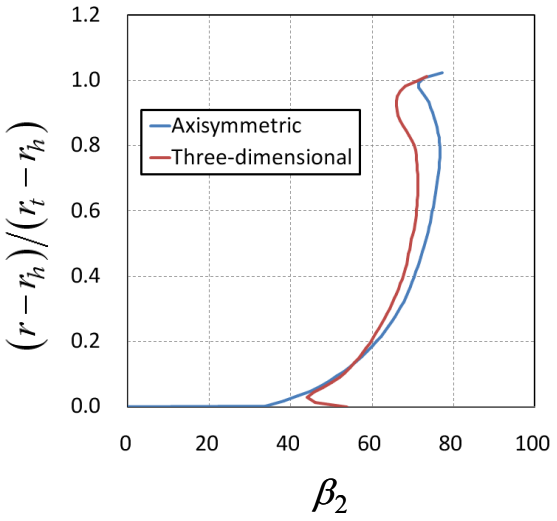

(b) Rotor outlet

Fig. 6 Spanwise distributions of relative flow angle for wind-lens turbine.

3.2 Half-ducted propeller fan

The present axisymmetric viscous flow modeling has been applied also to a half-ducted propeller fan. Its design specifications are shown in **Table 2**. As shown in **Fig. 3 (a)**, several separation regions are formed around this propeller fan. In consequence, it is difficult to predict flow distributions in the fan at its design process. For the axisymmetric viscous flow calculation, the distribution of the rotor blade loading was specified using numerical results of the three-dimensional flow calculation in the same way as the above wind-lens turbine. A computational grid for the axisymmetric viscous flow calculation is shown in **Fig. 7**. It has 32,568 computational cells; a computational grid for the three-dimensional flow calculation has 1,158,192 cells.

Spanwise distributions of the axial velocity at the inlet and outlet of the propeller fan rotor are presented in **Fig. 8**. The axial velocity is normalized by the rotor tip speed. There are great discrepancies between the axisymmetric and three-dimensional flow calculation results. It is obvious that the discrepancies result from the several separated flow structures shown in **Fig. 3 (a)**.

Figure 9 shows spanwise distributions of the relative flow angle at the fan inlet and outlet. Compared with the axial velocity distributions shown in **Fig. 8**, the relative flow angle distribution is well predicted for the fan inlet. Considering the importance of the inlet flow angle, the present flow modeling is suitable for the design use.

Table 2 Design specifications of half-ducted propeller fan.

Blade number	**11**
Rotational speed	**2400 [rpm]**
Rotor diameter	**320.0 [mm]**
Hub/Tip ratio	**37.5 [%]**

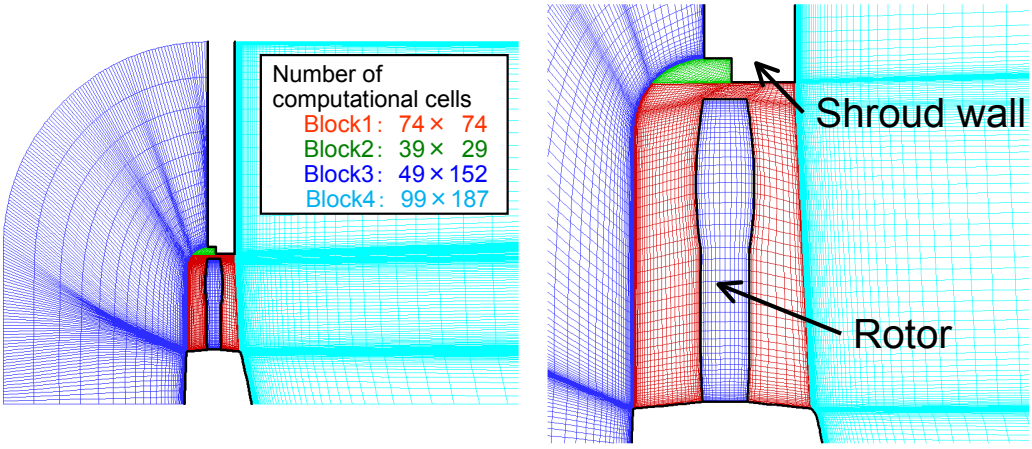

(a) Total view (b) Rotor region

Fig. 7 Computational grid for half-ducted propeller fan.

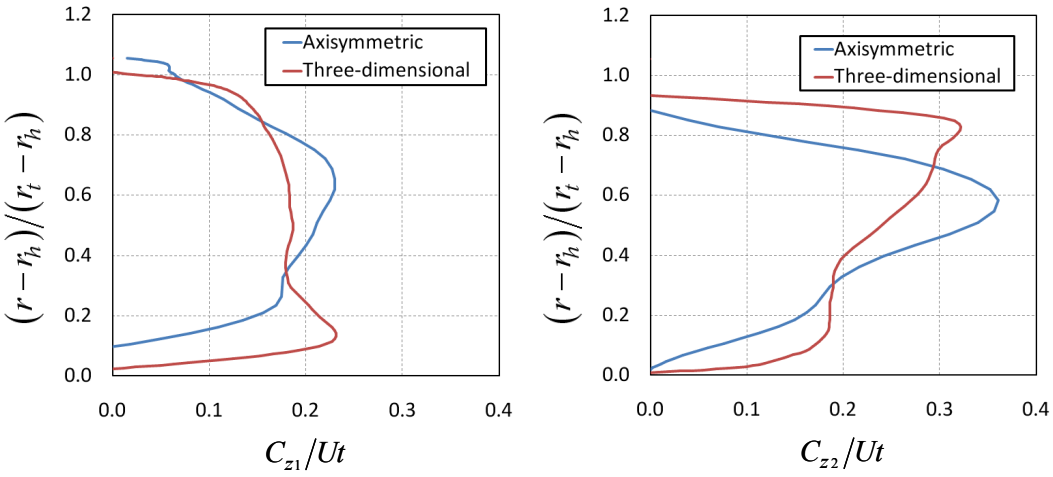

(a) Rotor inlet (b) Rotor outlet

Fig. 8 Spanwise distributions of axial velocity for half-ducted propeller fan.

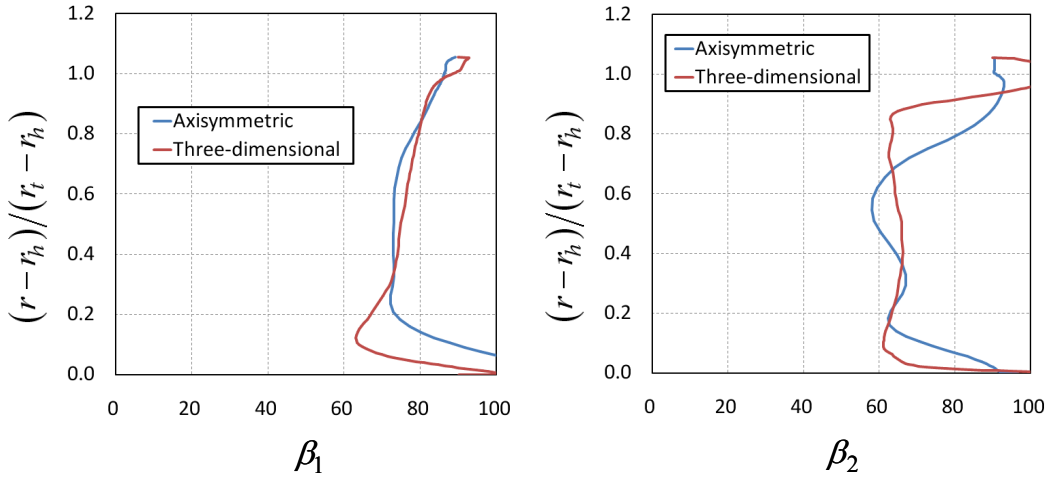

(a) Rotor inlet (b) Rotor outlet

Fig. 9 Spanwise distributions of relative flow angle for half-ducted propeller fan.

4. Concluding Remarks

An axisymmetric viscous flow modeling for the meridional flow calculation in the aerodynamic design of the half-ducted turbomachinery blade rows has been presented. It is assumed that the meridional flow is axisymmetric and viscous one. To take into account the blade loading on the assumption of the axisymmetric flow, a blade force is introduced as a body force to the axisymmeric Navier-Stokes equations. In the present modeling, the blade force contains the inviscid blade effect only, namely, the pressure difference between the pressure and suction surfaces of a blade.

Numerical examples have been presented for a wind-lens turbine and a half-ducted propeller fan in order to demonstrate the validity of the present flow modeling. For the wind-lens turbine, the present flow modeling can predict non-uniform flow distributions at the inlet and outlet of the turbine rotor. For the half-ducted propeller fan, however, the formation of the several separated and vortical flow structures results in the well prediction of the inlet flow angle only. It is found that the present flow modeling is suitable for design tool.

References

1) C. M. Jang, M. Furukawa and M. Inoue; Analysis of Vortical Flow Field in a Propeller Fan by LDV Measurements and LES: Part 1. Three-Dimensional Vortical Flow Structures, Transactions of ASME, Journal of Fluids Engineering, Vol. 123, No. 4, pp. 748-754 (2001).
2) C. M. Jang, M. Furukawa and M. Inoue; Analysis of Vortical Flow Field in a Propeller Fan by LDV Measurements and LES: Part 2. Unsteady Nature of Vortical Flow Structures due to Vortex Breakdown, Transactions of ASME, Journal of Fluids Engineering, Vol. 123, No. 4, pp. 755-761 (2001).
3) Y. Ohya, T. Karasudani, A. Sakurai and M. Inoue; Development of a High-Performance Wind Turbine Equipped with a Brimmed Diffuser Shroud, Transactions of the Japan Society for Aeronautical and Space Sciences, Vol. 49, No. 163, pp. 18-24 (2006).
4) S. H. Kim, M. Furukawa, M. Inoue and Y. Ohya; Three-Dimensional Flow Analysis around a Wind Turbine with Brimmed Diffuser, Proc. of the 7th Asian International Conference on Fluid Machinery, Paper No. 20022 (2003).
5) M. Furukawa and M. Inoue; Meridional Through-Flow Calculation Including the Effects of Non-Axisymmetric Flow in Turbomachinery, Memoirs of the Faculty of Engineering, Kyushu University, Vol. 46, No. 3, pp. 309-321 (1986).
6) M. Furukawa, T. Nakano and M. Inoue; Simulation of Transonic Cascade Flow Using an Unfactored Implicit Upwind Relaxation Scheme with Inner Iterations, Transactions of ASME, Journal of Turbomachinery, Vol. 114, No. 3, pp. 599-606 (1992).
7) M. Furukawa, M. Yamasaki and M. Inoue; A Zonal Approach for Navier- Stokes Computations of Compressible Cascade Flow Fields Using a TVD Finite Volume Method, Transactions of ASME, Journal of Turbomachinery, Vol.113, No.4, pp.573-582 (1991).
8) D. C. Wilcox; Reassesment of the Scale-Determining Equation for Advanced Turbulence Models, AIAA Journal, Vol. 26, No. 11, pp. 1299-1310 (1988).
9) M. Furukawa, K. Saiki and M. Inoue; Numerical Simulation of Three-Dimensional Viscous Flow in Diagonal Flow Impeller, ASME FED, Vol. 227, pp. 29-36 (1995).